Recent, rapid restructuring of North American bumble bee communities is associated with climate warming

Jeremy Hemberger[1] *, Neal Williams[1]

[1] Department of Entomology and Nematology, University of California Davis. One Shields Ave, Davis, CA 95616 USA

* Corresponding author address: Department of Entomology, University of Wisconsin-Madison. 1630 Linden Dr, Madison, WI 53706

Phone: (608) 622-2698

Email address: j.a.hemberg@gmail.com

Abstract

A rapidly warming climate has become one of the primary forces driving changes in biodiversity worldwide. The impact of warming temperatures on insect communities is of particular interest given their importance for ecosystem function and service provision and the uncertainty around whether insect communities can keep pace with the rate of increasing temperatures. We use a long-term dataset on bumble bee species occurrence and data on summer maximum temperature trends across North America to characterize community-level responses to recent climate warming. Bumble bees are relatively well recorded historically and are sensitive to warming temperatures. We examined responses using the community temperature index (CTI) – a measure of the balance of cool- and warm-adapted species within local communities. Starting in 2010, bumble bee average CTI across North America has rapidly increased after a period of slight increase from 1989 to the late 2000s. This increase is strongly associated with recent increases in maximum summer temperatures. The increase in CTI is spatially extensive, occurring throughout North America, but the areas of greatest concern include mid to high latitudes as well as low and high elevations - areas relatively shielded from other intensive global changes (e.g., land-use). On average, bumble bee CTI has increased 0.99°C from 1989 to 2018, a change of similar magnitude to the increase in maximum summer temperatures. The rapid shift in bumble bee communities appears to be at pace with shifting summer temperatures, with an approximate, equivalent northward shift of ~104 km from 1989-2018 for both. This indicates an adaptive capacity among some bumble bee species. However, warming temperatures are also likely reducing the occurrence and local abundance of cool-adapted species that may serve important ecological roles within their range. Our results provide strong evidence of the pervasive impacts posed to insect communities by temperature increases in the past few decades.

Introduction

Climate change is driving profound changes in animal occurrence and community composition worldwide. Long-term increases in average temperature as well as increases in acute, extreme weather events (e.g., heat waves) have been linked to both positive (Kammerer et al., 2021; Crossley et al., 2021) and negative outcomes for biodiversity (Kammerer et al., 2021; I. Oliver et al., 2016; Outhwaite et al., 2022; Sirois-Delisle & Kerr, 2018). Regardless of the direction of such outcomes, a rapidly changing climate has the potential to fundamentally alter biological processes, including ecosystem services that maintain biodiversity and support global agricultural production (Johnson et al., 2023; Settele et al., 2016).

Insect responses to climate change are of specific interest given the growing documentation of declines in a variety of taxa and regions (Halsch et al., 2021; Raven & Wagner, 2021). Although several anthropogenic drivers of global change are at play (J. Hemberger et al., 2021), a changing climate is particularly menacing given the number of potential direct and indirect impacts it has on insects and its capacity to be a force-multiplier, interacting with other factors to exacerbate changes in insect populations (Hoover et al., 2012; Forrest et al., 2018; Kenna et al., 2023). Like many global change drivers, rapidly increasing temperatures may favor some species while leading to local extirpations of others. Though temperatures above the critical limits of species (e.g., CT_{max}; Oyen et al., 2018) are unlikely, the extent to which climate warming has contributed to local shifts in insect abundance and species' range remains mostly unknown - placing a host of ecological processes and services in limbo.

Even among the most studied insect taxa there is debate about the extent, severity, and direction of effects associated with climate change. Bumble bees are a prime example with some studies revealing extensive declines (Soroye et al., 2020; but see Guzman et al., 2021) and others suggesting resilience and relative stability (Guzman et al., 2021; Maebe et al., 2021) or mixed patterns of decline and increases over time(Jackson et al., 2022). Most current approaches examining the long-term influence of climate on bumble bees use occupancy models to relate changes in species occurrence to trends in climate, such as increases in temperature and changes in precipitation (Janousek et al., 2023). Although this method can yield valuable insights, it can be challenging to align the framework with the incidental and imperfect occurrence data that abounds in large-scale insect databases, making model outcomes sensitive to occupancy assumptions (Guzman et al., 2021). Moreover, the occupancy approach framework does not capture the physiological mechanisms driving species responses to warming temperatures. As such, a more thorough understanding of where/when insects are most impacted by climate change requires exploring alternative analytical methods that better tie climatic changes to estimates of insect physiological preferences and limits.

We characterize bumble bee community responses to recent climate warming at the continental scale by examining changes in the community temperature index (CTI), a physiological metric of community responses to climate based on the composition of cool- and warm-adapted species. This metric can be used to assess the rate of change in community composition based on historical species temperature preferences (species temperature index, STI), as well as the spatial velocity of community changes (Devictor et

al., 2008, 2012). When examined over time along with temperature, CTI can help determine whether species are keeping pace with the velocity of temperature trends (i.e., an increase in warm-adapted species and a loss of cool-adapted species in rapidly warming areas; Fourcade et al. 2019), or whether communities are accruing "climate debts", as rising temperatures outpace species turnover (Devictor et al., 2012).

Using 50 years of records from the Bumble bees of North America database (Richardson 2023), we test for changes in bumble bee communities using CTI across North America and quantify CTI shifts' association with trends in maximum summer temperatures. Specifically, we wanted to address the following questions: (1) is there evidence of an increase in bumble bee CTI over time? (2) are changes in CTI associated with increases in summer temperatures? (3) are CTI changes greater in areas particularly vulnerable to a changing climate (e.g., higher latitudes and elevations)? (4) are the observed shifts in CTI keeping pace with the rate of temperature increases (i.e., are communities accruing "climate debt") and (5) which species are driving any observed changes in CTI? We predicted a steady increase in bumble bee CTI in accordance with documented increases in average maximum summer temperatures over the past century and that changes would be more dramatic at higher latitudes and elevations. We also expected that a host of common species that have increased in occurrence over the past several decades would be the strongest drivers of change in CTI across the continent.

Methods

North American bumble bee occurrence and community data

We used occurrence records for 59 species of North American bumble bees from the bumble bees of North America database (BBNA; **Richardson 2023**). This database composes 781,280 records from 1805-2020 from a variety of sources (e.g., natural history collections, research studies, citizen science programs). Because the database consists of an amalgam of sources, we took several steps to account for known biases (Bartomeus et al., 2019; Gotelli et al., 2021). The species and community temperature indices at large scales of our analysis are robust to imprecision in the underlying distributional data (Devictor et al., 2008); nonetheless we filtered the original dataset to include only complete records (i.e., identified to species, containing complete coordinates) and unique collection events (distinct combinations of species, date, coordinates, and observer; Figure S1A). This step helps to minimize the bias associated with unequal sampling efforts and differential data collection methods across all observers. Moreover, we conducted a range of sensitivity analyses (see below) to determine whether our results were robust given our assumptions and methodological decisions.

Is there evidence of an increase in bumble bee CTI over time?

Calculating the CTI first requires the species temperature index (STI; i.e., the historical average summertime temperature experienced over a species' approximate range; Figure S1B) to be calculated. We used a subset of occurrence records from 1970-2000 to extract historical summertime temperature associations and calculate the STI for each species. In this, we assumed that the records contained within this period are representative of the entire range of each species. Using the raster package (Hijmans, 2023), we extracted temperatures at the specific location (i.e., raster pixel) of each occurrence record from the raster of average historical maximum summer temperatures using WorldClim version 2.1 historical climate data for maximum monthly temperatures at 30 arc-second (~1 km2) resolution (Fick & Hijmans, 2017). To create a raster of historical maximum summer temperatures, we calculated the average maximum monthly temperature for summer months (defined here as June-September) for a historical period of 1970 to 2000. We then used this raster to extract STI values using our bumble bee occurrence records.

Our analysis framework required us to assign records to communities to calculate CTI for given locations/times (Figure S1C. Although the species assemblages we define below are considerably larger than the scale of an ecological community, the analysis is ultimately agnostic to this point, and it does not affect our specific questions. We refer to them as communities/CTI to maintain consistency with the existing literature. Also, because we used occurrence records from a variety of sources whose spatial locations varied over time, using fixed sampling locations was not possible. Instead, we created a hexagonal grid across North America at a broad spatial scale (50 km hexagonal grid resolution, center to side: ~ 6600 km2) to act as stand-in "community" boundaries. We chose a 50 km resolution to ensure we would capture sufficient records within each grid cell to robustly estimate the broad spatiotemporal trend of CTI (Jackson et al., 2022). To determine if the resolution of our grid cells impacted our results, we also conducted our analyses using 10 and 100 km center-to-side hexagonal grid cells. We assigned bumble bee occurrence records to each

grid cell to create quasi-communities, requiring each cell to contain at least 2 species for a given year to calculate CTI. We used hexagonal grid cells to minimize possible edge effects and provide a better fit across the curvature of the earth at large spatial scales (e.g., continental; Birch et al. 2007).

Using STI values, we then calculated CTI within each grid cell where at least 2 species records were present in the grid using the full set of bumble bee occurrence records from 1961-2018 (Figure S1D. We calculated CTI using two different methods, first using occurrence records for species *i* occurring within a given community (grid cell) *j*

$$Equation\ 1: Occurrence\ CTI_j = \frac{\sum_{i=1}^{n} STI_{i,j}}{n}$$

and then using abundance weighted estimates of species within each community:

$$Equation\ 1: Occurrence\ CTI_j = \frac{\sum_{i=1}^{n} STI_{i,j}}{n}$$

where $a_{i,j}$ is the abundance of species *i* at site *j*, and *n* is the total number of species within a grid cell (Princé & Zuckerberg, 2015). These two approaches, though similar, estimate the two mechanisms of change in CTI. Using occurrence records (Equation 1) allowed us to test shifts in CTI due to changes in occurrence (i.e., immigration/extirpation), while calculating CTI using abundance weighting (Equation 2) allowed us to understand shifts in CTI as a function of changes in local relative abundance (i.e., species becoming more common/rare within a given community).

Are changes in CTI associated with increases in summer temperatures?

To determine long-term warming trends across North America, we used WorldClim gridded historical monthly weather data from 1961-2018 for our defined summer months (Fick & Hijmans, 2017). First, we averaged the maximum monthly temperature for each year. Second, we extracted the mean maximum temperature within each of the bumble bee community grid cells (Figure S1E). This procedure created a time series of the average maximum summer temperature for each year/grid cell from 1961-2018. Third, we calculated the average maximum summer temperature for a historical period from 1961-2000 for each grid cell; this is our baseline, and we refer to it as the temperature "normal". Last, we calculated the summer maximum temperature anomaly (defined here as the deviation from long-term normal) and averaged these using 3 moving-window scales of 3, 10, and 30 years to capture metrics of relatively short-, medium-, and long-term changes in maximum summer temperatures, respectively. To illustrate the estimated trends in maximum summertime temperatures, we calculated the change in our 3 scales of anomalies by subtracting the 1989 average anomaly (first possible year to calculate 30-year average) from the 2018 average anomaly for each grid cell.

We used generalized additive models (GAM) to quantify trends in CTI over space and time and determine whether changes in CTI were related to short-, medium-, and long-term trends in temperature anomalies (Figure S1F). Generalized additive models provide a highly flexible computational framework to account for variable trends in spatiotemporal processes (Pedersen et al., 2019) and are especially well-suited for the analysis of

potentially complex time series and can readily identify periods of significant change (Simpson, 2018).

For each measure of CTI (occurrence and abundance-weighted), we fitted a GAM to model the effects of spatial location (latitude, longitude, and elevation), long-term trend (year), short-, medium-, and long-term estimates of rising temperatures (3, 10, and 30-year summertime maximum temperature anomalies). For the remainder of this manuscript, we refer to this GAM as the global model.

$$Equation\ 3: CTI_j \sim s(lat, long) + s(year) + s(elevation) + ti(lat, long, year, elevation) + s(eco\ region, bs = \text{"re"}) + \mathrm{s}(\bar{T}_{\max 3}) + \mathrm{s}(\bar{T}_{\max 10}) + \mathrm{s}(\bar{T}_{\max 30})$$

We fit the model using the mgcv package in R (Wood, 2011). The goal of each model was to identify any temporal trends in CTI and determine where and when significant changes have occurred. Because of the differences in geography, land-use, and climate across North America, we included a 2-dimensional smooth of latitude and longitude, and we allowed the estimated temporal trend in CTI to vary according to spatial location by including a tensor product interaction of latitude, longitude, elevation, and year (Equation 3). We also included a random effect smooth of ecological region (level 1) to further account for variation in the response of CTI in accordance with common biophysical characteristics within ecological regions, such as commonalities in vegetation and other climate variables (e.g., precipitation). We included smooths of 3-, 10-, and 30-year summertime maximum temperature anomalies to determine whether changes in CTI were correlated with trends in warming maximum summer temperatures. Including three different anomaly scales allowed us to assess the temporal scale of temperature change bumble bee communities respond most strongly to. This model was fit to CTI estimates from 1989-2018 because 1989 was the first year for which 30-year temperature anomalies could be calculated. We tested the model for spatial and temporal autocorrelation in the residuals. For spatial autocorrelation, we tested simulated residuals with a Moran's I test using the DHARMa package (Hartig, 2022). For temporal autocorrelation, we visually examined the autocorrelation function using scaled, simulated residuals.

To visualize the change in CTI over time, we generated CTI predictions across the spatial and temporal extents of our dataset using the global model for each grid cell. We then determined the change in CTI from 1989-2018 by subtracting the CTI estimate for 1990 from that of 2018 for each grid cell. To visualize model uncertainty, we calculated the average standard error of global model predictions for each grid cell from 1990-2018. We visualized the effect of the three moving-average temperature anomalies on CTI by plotting the partial effects (prediction of CTI as a function of temperature holding other variables are at their mean value) of each anomaly from the global model using the gratia (Simpson, 2023) package.

Are CTI changes greater in areas particularly vulnerable to a changing climate (e.g., higher latitudes and elevations)?

To determine whether CTI changes were most drastic (i.e., greater slope in fitted GAM) in areas known to be experiencing accelerated climatic changes, we examined the rate of change in the slope (i.e., first derivative) of our fitted model smooth (Fig. S2). To do this, we first fitted a GAM to CTI predictions with a single smooth of year to create a spatially

explicit, estimated trend of CTI for each grid cell. Then, for each grid cell's fitted GAM year smooth, we extracted the first derivative with respect to time (1990-2018) using the derivatives() function from the gratia package (Simpson, 2023). For elevation and latitude, we calculated the mean derivative value for each grid cell (i.e., the average rate of change of the CTI of a grid cell from 1989-2018) and then plotted this against the mean elevation and latitude of the grid cell. We visualized the relationship with a GAM fit using the geom_smooth() function in the ggplot (Wickham et al., 2019) package. To determine whether CTI changes were consistent or have accelerated over time, we calculated the derivative values for the year smooth for each grid cell and plotted these values against the year. Like elevation, this relationship was visualized with a simple GAM fit.

Are the observed shifts in CTI keeping pace with the rate of temperature increases (i.e., are communities accruing "climate debt")

By calculating the ratio of the temporal rate of change in CTI (i.e., how much is CTI changing per year) with that of the spatial rate of change (i.e., how much is CTI changing per degree of latitude), we can approximate the velocity of the northward shift for bumble bee communities (°C yr-1/°C km-1 = km yr-1). This metric provides an approximation of how much communities have effectively shifted northward in terms of their composition (Devictor et al., 2008, 2012) A similar procedure can be performed to calculate the spatial velocity in temperature. We estimated the rates of change for CTI over time by calculating the average derivative value of the "year" smooth in the model. For the spatial trend, we fit a GAM to the model predictions of CTI and related these to a single smooth of latitude and then calculated the average derivative value of the "latitude" smooth. We compared the approximate spatial velocities of CTI and temperature to determine whether there is a lag between the shifts in temperature and the communities' response. A lag would indicate that temperatures are increasing faster than communities are able to respond, thus accruing "climate debt".

Which species are driving any observed changes in CTI?

Although quantifying the trend in CTI provides evidence for whether communities are being restructured in response to a changing climate, the procedure does not implicitly identify which species are responsible for driving any observed increases. To address this, we used a jackknife analysis (Princé & Zuckerberg, 2015), iteratively eliminating one species from our model dataset and refitting the global model. For this analysis, we filtered to the grid cells that were within the range of the given species. The range was determined by creating a convex hull around all species occurrence records used in STI calculations and extracting the grid cells within this estimated range. To determine whether a species contributed to the trend in CTI, we fit a GAM with a single smooth of year to the predicted CTI values of grid cells within a species' range and then calculated the percent difference between the mean first derivative of the fitted year smooth in the reduced model predictions to that of the global model predictions. In this context, a positive percentage change indicated that a species had a positive contribution toward the CTI trend (i.e., the average slope of the year smooth increases when the species is included). That is, either more occurrences, or an increase in the local abundance of this species leads to an increase in CTI. Conversely, species with a negative percent change had a negative contribution

toward the CTI trend; as those species occur less frequently or decrease in local abundance, the CTI trend should increase.

Model validation

We performed cross validation on our global model using testing data that was filtered out of the full BBNA database. These collection events, while not "unique" (i.e., not necessarily fully independent given our strict definition), were still valid records that could be used to calculate the CTI for any given location. Upon calculating the CTI for grid cells using these records, we compared the values against predictions from the global model by using the coefficient of determination (R2), root mean square error (RMSE) and mean absolute error (MAE).

Despite the vast number of individual occurrence records within our dataset, there were many grid cells that did not contain species occurrence data for fitting the model. Given that we explicitly model CTI over space, we presented our results above using predictions within all grid cells given the strength of our global model fits. However, we also assessed the results when using model predicted values of CTI only for grid cells containing occurrence data. This approach was primarily meant to provide conservative estimates of CTI changes, particularly where in space (i.e., latitude, elevation) and time changes were greatest.

We conducted all data wrangling, GIS operations, modeling, and visualization using R (R Core Team, 2017) using the aforementioned and following packages: tidyverse (Wickham et al., 2019), raster (Hijmans, 2023), sf (Pebesma, 2018), performance (Lüdecke et al., 2021), janitor (Firke, 2021), paletteer (Hvitfeldt, 2021), exactextractr (Daniel Baston, 2022), foreach (Microsoft & Weston, 2022), and data.table (Dowle & Srinivasan, 2023) packages.

Results

Bumble bee community temperature index has increased across a majority of North America

From 1989-2018 bumble bee CTI increased substantially across most of North America, but the magnitude of change was spatially variable - with an overall average increase of 0.99 ± 1.98 °C (mean ± SD) and a range of a decrease of 6.30 °C to an increase of 7.99 °C (Fig. 1A). The predictions were most certain across the coterminous United States where there is a high density of bumble bee records and less certain in the most northern grid cells of our study region in the high Tundra and Queen Elizabeth Islands as well as in the tropical wet forests of Mexico (Fig. 1B). The spatial trends of the increase in CTI were nearly identical between occurrence and abundance-weighted CTI; however, changes in occurrence CTI were marginally smaller (0.78 ± 1.75 °C). The global model, which quantified the change in CTI as a function of space, time, and changes in short-, medium-, and long-term temperature increases, explained a substantial portion of the deviance in both the abundance-weighted (Table S1; 86.0%, adj-R^2 = 0.849) and occurrence models (Table S1; 86.3%, adj-R^2 = 0.851).

The results of our analysis were consistent irrespective of the grid scale used in aggregating communities (Fig. S3; Table S2). The exception was in areas of British Columbia and Alaska where a highly concentrated spatial pattern of bumble bee records likely led to a predicted decrease in CTI in grid cells when aggregated at the 50 and 25 km grid scale. Aggregating at the largest scale (100 km center-to-side hexagonal grid) revealed the most wide-spread increases in CTI, with nearly all grid cells exhibiting an increase in CTI from 1989 to 2018.

Our models performed well when cross-validated using withheld data from the BBNA database (Fig. S4). Coefficient of determination (R^2) values ranged from 0.79-0.81, root mean squared error (RMSE) ranged from 1.22-1.31, and mean absolute error (MAE) ranged from 0.91-0.96. In addition, our model performance was consistent across the three tested grid scales. Predictions were most accurate for CTI values ranging from 23-28°C which corresponded to the regions where the bulk of the occurrence records were collected. Prediction accuracy was most variable among cool regions in the north and sub-arctic (CTI < 23°C).

Shifts in CTI are strongly related to long-term increases in summer temperature

Summertime maximum temperatures have increased by 1989-2018 (Fig. 1C-E), with increases most apparent at 10- (0.630 ± 0.405 °C) and 30-year average anomalies (0.969 ± 0.342°C; Fig. 1D, E; Fig. S5). Increases in the 30-year summertime maximum temperature anomaly showed a strong statistical association with increases in bumble bee CTI (Fig. 2C; $F = 4.561$, $p = 0.002$). Increases in the 30-year temperature anomaly between 0-0.5°C had no impact on CTI. However, increases beyond 0.5°C were associated with a rapid increase of up to 1°C in bumble bee CTI (partial effect due solely to 30-year temperature anomaly). Of the 2,425 grid cells, 1,753 exhibited parallel increases in change in CTI and the change in the 30-year temperature anomaly between 1989-2018 (Fig. 3A). Beyond a 1°C change in the 30-year temperature anomaly the changes in CTI rapidly increase, with gains of 1 to 6.8°C. The relationship of CTI with short term, 3-year moving average shifts in summer

temperature anomalies, while statistically supported, was weak and variable over the range of the anomalies (Fig. 2A; F = 2.584, p = 0.032). There was no statistically supported relationship between the 10-year average anomaly and bumble bee CTI (Fig. 2B; F = 0.064, p = 0.802).

CTI is increasing fastest at low and high elevations, latitudes, and more recent years

We examined patterns in the rate of change in CTI across the continent to determine where and when the most extreme changes in CTI were occurring and whether these areas overlapped with areas known to be heavily impacted by a warming climate (Janousek et al., 2023). The rate of change in CTI was greatest at low (< 800 m) and high elevations (> 2000 m; Fig. 4A) and increased with increasing latitude (Fig. 4B). Moreover, the rate of change in CTI has increased from 1989-2018, with CTI increasing most rapidly after 2010 (Fig. 4C). These results varied slightly when analyzed with predictions from only grid cells containing occurrence records, with changes in CTI being greatest at high elevations (Fig. S6A; > 2000 m) and mid-high latitudes (Fig. S6B; 35 – 60°). The temporal patterns of the rate of change were largely similar but were positive only from 2003 and beyond (Fig. S6C), confirming the accelerating rate of CTI change from 2010 onward that is exhibited when using predictions from all grid cells (Fig. 4C).

Bumble bee community changes are keeping pace with climate warming

The spatial velocity of bumble bee CTI increases (3.58 km yr-1) was nearly identical to that of summer temperature increases (3.59 km yr-1). Over the course of the study (29 years), bumble bee communities and summer temperatures have exhibited an equivalent northward shift of approximately 104 km. This comparison, while highly dependent on the complexity of the GAM smooths used to estimate the spatial and temporal trends, indicates that shifts within bumble bee community composition are effectively keeping pace with the rate of climate warming.

Species contributions to changes in CTI

All but 3 species had positive contributions toward the mean derivative of the temporal trend in bumble bee CTI from 1989-2018 (Table S3). Of the most represented species in the dataset, *B. occidentalis* (% change = 70.42%), *B. nevadensis* (% change = 69.65%), *B. ephippiatus* (% change = 66.87%), *B. bifarius* (% change = 66.71%), and *B. vosnesenskii* (% change = 64.32%) had the greatest contribution for both abundance-weighted and occurrence CTI trends. Of the top 25 contributors to the increase in CTI, 14 (56%) are in the subgenus Pyrobombus (and 3 of the top 5). In general, species with wider ranges and more variable STI tended to be those that had the biggest contributions toward the long-term increase in CTI.

Discussion

We documented significant, spatially extensive shifts in the thermal tolerance of species within North American bumble bee communities in response to long-term increases in summer temperatures. Over the last 29 years across the continent, bumble bee community assemblages increasingly consist of either more warm-adapted or fewer cold-adapted species, with increases in community temperature index, the measure of the balance of warm- and cool-adapted species, most pronounced at mid- to high latitudes, and high elevations in the American Rockies, Intermountain West, and central Mexico. The community temperature index increased according to both occurrence and abundance-weighted indices, suggesting that shifts in both local abundance and broader changes in species occurrence (i.e., range shifts) underlie the changes in community composition. The rapid shift in bumble bee communities appears to be on pace with shifting summer temperatures, with an approximate, equivalent northward shift of ~104 km from 1989-2018 for both CTI and temperature. Our work provides additional evidence of the pervasive impacts a warming planet has for insect biodiversity and identifies regions of concern where anthropogenic climate warming is rapidly restructuring the communities of an ecologically important group of insects.

An increase of warm-adapted species within biological communities is a logical consequence of a rapidly warming climate (Tingley & Beissinger, 2013). Similar shifts have been observed in bird communities in response to both warming summer (Devictor et al., 2008, 2012) and winter (Princé & Zuckerberg, 2015) temperatures. Because insects are ectotherms, temperature-induced shifts in range and abundance may be even more pronounced. Indeed, large changes in insect CTI have been observed for both bumble bees (Fourcade et al., 2019) and butterflies (Devictor et al., 2012); however, trends in CTI are often not explicitly tied to spatial and temporal patterns of warming temperatures. Our results provide this link and show a clear statistical relationship between increases in CTI and long-term increases in maximum summer temperatures across North America, with areas experiencing a 30-year temperature anomaly of greater than or equal to 0.5°C strongly associated with a rapid increase in bumble bee CTI. These results identify areas of ample concern where rates of bumble bee community change and summer temperature increases are the greatest (Fig. 1; dark orange and red areas).

The frontline of species' responses to climate have tended to be at high latitudes and elevations. Northern regions have experienced rapid increases in temperature leading to pronounced phenological shifts across taxa (Parmesan, 2007). Our results support this trend, finding greatest rates of bumble bee CTI change at higher latitudes and high elevation. The bumble bee species in these locations tend to have narrower ranges and be cold-adapted, traits identical to other insect taxa that have exhibited declines due to climate (Engelhardt et al., 2022; Halsch et al., 2021; Neff et al., 2022). The rapidly increasing CTI, particularly at high elevations, suggests that cold-adapted species are being displaced by warm-adapted, low-elevation species. This phenomenon has been observed in the US Rocky Mountains where bumble bee communities are increasingly dominated by low-elevation species using high-elevation habitats as a thermal refugia (Miller-Struttmann et al., 2022). An upslope range expansion appears to be a common response of bumble bee communities to warming temperatures rather than expansions of northern ranges (Kerr et

al., 2015; Sirois-Delisle & Kerr, 2018). Despite the rapid changes observed at higher latitudes, biological communities in southern latitudes and lower elevations are not protected from a changing climate (Dillon et al., 2010), and we documented some shifts in CTI in central Mexico and at low elevations. That said, if species lost from communities have STI values comparable to those species remaining, large shifts in CTI may be effectively masked, highlighting a limitation of our approach.

An increase in CTI could be the result of two mechanisms. First, shifts in the occurrence of bees within a community (i.e., immigration/extirpation of warm-/cool-adapted species via range expansion/contraction) and second, changes in the local abundance of warm-/cool-adapted species. We found evidence supporting both mechanisms by modeling occurrence and abundance-weighted measures of CTI. Shifts in local relative abundance align with existing research (Cameron et al., 2011; J. Hemberger et al., 2021); however, substantial range expansion of warm-adapted bumble bees has not been described (Kerr et al., 2015) and may be unlikely given bumble bee dispersal capacities Fijen (2021). That said, select species of bumble bees may be capable of long-distance dispersal (Fijen, 2021), and significant range shifts observed in other insect taxa have been observed (Warren et al., 2001; Hinckling.2005). Regardless, our jackknife analysis revealed that the largest contributors to increasing abundance and occurrence-based CTI within their range are common species that have exhibited both range increases (Looney et al., 2019; e.g., B. impatiens Palmier et al., 2019) and increases in local abundance. This result indicates that certain species are sensitive to and more capable of effectively tracking/adapting to ideal climatic conditions (Maebe et al., 2021). The equivalent, northward spatial shift in bumble bee community composition that we observed was nearly identical to that of the spatial shift in maximum summer temperatures. This result provides further evidence that, at least some species, are successfully tracking warming climates and not accruing climate debts (Devictor et al., 2012). However, other species (e.g., *B. occidentalis*) are not able to successfully track warming and are likely to suffer substantial reductions in range as a result (Janousek et al., 2023). Such contrasts highlight the species-specific nature of bumble bee responses to a rapidly changing climate (Jackson et al., 2022; Whitehorn et al., 2022). Additional research is needed detailing species-specific responses to warming conditions – focusing on identifying the physiological and evolutionary mechanisms that drive species' plasticity to changing environmental conditions.

An increase in the occurrence and abundance of warm adapted species does suggest a physiological/climate preference mechanism is at play (i.e., direct effect). Several studies document significant, direct effects of warming on insect pollinators (CaraDonna et al., 2018; Hemberger et al., 2023; Kenna et al., 2021), however indirect effects mediated through biotic interactions may be just as if not more important (Ockendon et al., 2014). In the context of our study, such indirect effects imply that shifts in bumble bee community composition are occurring in part in response to climate-induced changes in the resource landscape (i.e., indirect effects). For example, warming climates can widen the temporal availability of resources due to earlier snowmelts, which in turn lead to an increase in bumble bee abundance (Ogilvie et al., 2017). Warming may also create phenological mismatches that reduce available forage for bees (Pyke et al. 2016, but see Bartomeus et al., 2011). Similarly, an increase in hot, dry summer conditions can significantly reduce floral resources and the bumble bees that depend on them (Iserbyt & Rasmont, 2013), and

similar patterns have been observed for butterflies (Crossley et al., 2021). Unfavorable conditions, often a result of extreme weather events such as heat waves and droughts, can create resource bottlenecks that have the potential to lead to population declines and local extirpation (Maron et al., 2015). Heat waves, for example, are expected to increase significantly in the coming century (Lopez et al., 2018; Meehl & Tebaldi, 2004; Thompson et al., 2022). As our study could not differentiate between direct and indirect pathways, parsing their relative impacts on bumble bees and other taxa is a critical research need. In the meantime, supporting bumble bees in the face of both direct and indirect effects may be accomplished by maintaining climate refugia, such as heterogeneity in vegetation structure, that can provide microclimatic respite from temperature extremes to bees (Pincebourde & Woods, 2020) and other taxa (e.g., birds, Kim et al., 2022) in addition to increasing spatial/temporal resource continuity to minimize negative indirect effects (Maron et al., 2015).

Given the spatiotemporal extent of our study, it is likely that warming summer temperatures and the temperature profile of a given bumble bee assemblage may co-vary with other, known factors of bumble bee community composition and occurrence. For example, losses in certain species across their range may be linked to disease Szabo et al. (2012). Additionally, at large-scales, a loss of suitable habitat via land-use intensification and change is also of concern. However, when examined together with shifts in land-use, climatic variables (and their associated indirect effects) tend to have as much or more power to explain long-term species trends than land-use or resource availability in bumble Kerr et al. (2015) and other wild bee species (Duchenne et al., 2020). Moreover, the areas of greatest increase in CTI are in areas removed from the most significant effects of land-use change (e.g., high latitudes and elevations; Halsch et al. 2021). Regardless, managing habitat offers a critical tool that can be used to mitigate the impacts of a changing climate (Kim et al., 2022; Oliver et al., 2016; Oliver et al., 2015; Outhwaite et al., 2022).

Conclusions

Climate change is poised to have significant, cross-scale impacts on insect behavior, populations, and communities (Halsch et al., 2021; Høye et al., 2021; Lehmann et al., 2020; Raven & Wagner, 2021). In this paper, we document a substantial shift in the functional composition of bumble bee communities with respect to climate that is tied to a long-term increase of summer temperatures in North America. Due to changes in both occurrence and abundance, several species within bumble bee communities appear to be tracking climate warming, however this is likely at the expense of other species that lack the adaptive capacity to cope with rapidly climbing temperatures. Although the exact mechanisms of these community-level shifts remain unknown (i.e., direct vs. indirect effect of warming), our work adds to a growing body of evidence that suggests climate change will result in many climate losers with unknown consequences for ecosystems. It is critical that we focus on designing adaptation measures, such as climate refugia and climate-focused habitat conservation, to help combat the ongoing direct and indirect impacts a rapidly warming planet threatens. However, such efforts will only be successful in conjunction with substantial decreases in emissions (Oliver et al., 2015) – an essential solution to safeguard the planet's biodiversity for generations to come.

505 # Acknowledgements

506 # Data access

507 All data and R code for analyses are available on FigShare via LINK (data) and LINK (code)
508 and will be made public upon publication of this manuscript.

Figures and Tables

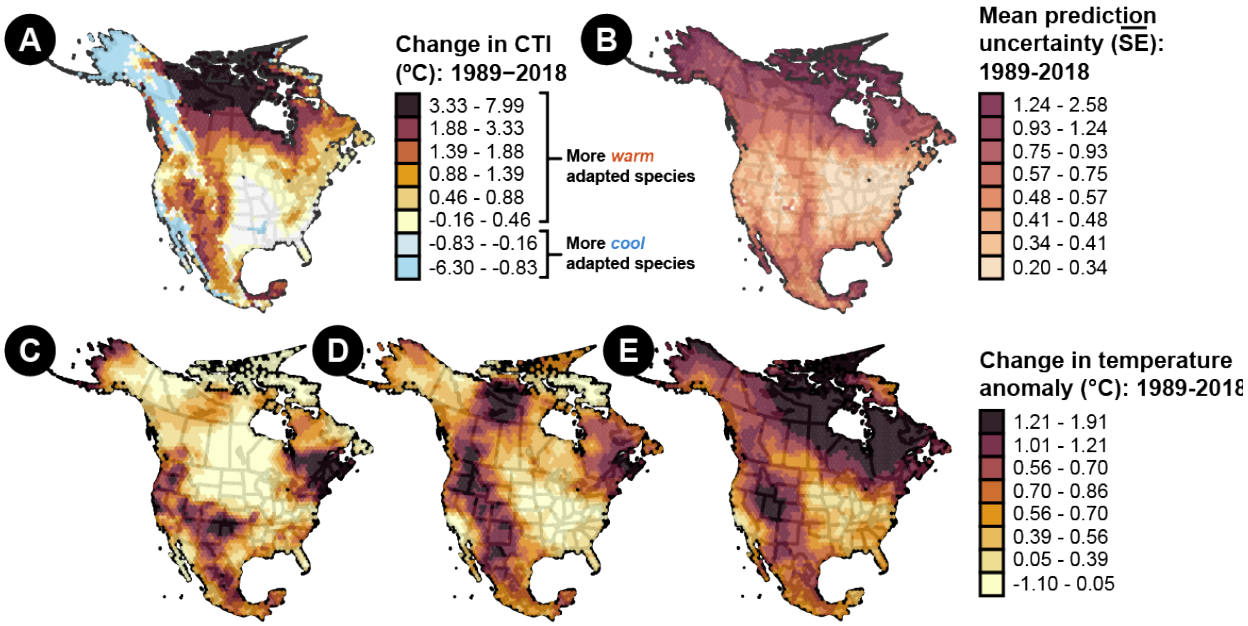

Figure 1: (A) Extrapolated spatial projection of the estimated change in community temperature index from 1990-2018 across North America. Differences in CTI were calculated for each grid cell by subtracting the model predicted CTIt = 1989 from predicted CTIt = 2018. (B) Spatial projection of the mean uncertainty estimates across years from 1989-2018. (C) Spatial projection of the change in the 3-year, 10-year (D) and 30-year (E) average temperature anomaly. Differences were calculated by subtracting the 1989 anomaly from the 2018 anomaly for each grid cell. Hexagonal grid cells are 100 km from side to side (~8600 km2).

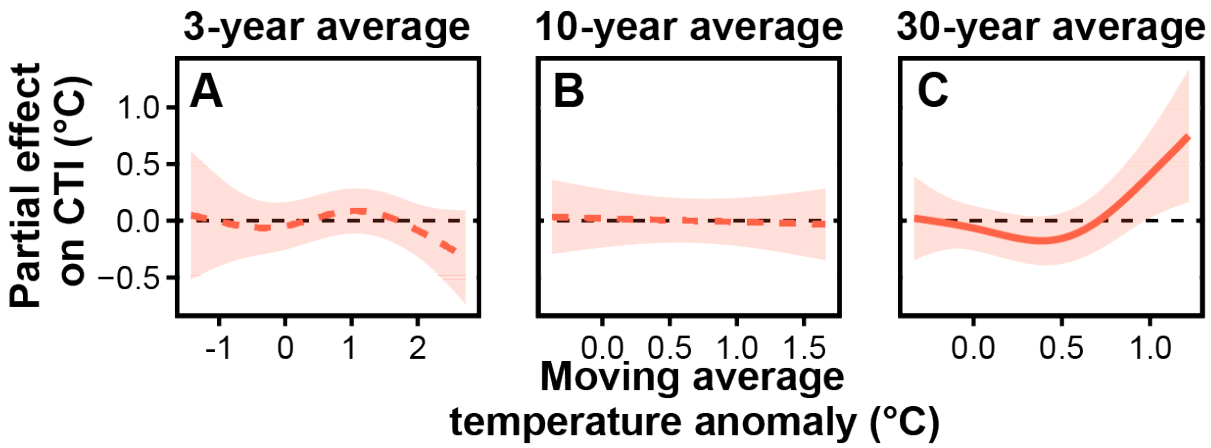

519

520 **Figure 2:** Generalized additive model partial plots (i.e., marginal effects) show the model
521 predicted effect of (A) 3, (B) 10, and (C) 30-year moving average temperature anomalies on
522 the community temperature index. Positive values on the y-axes indicate an increase in CTI,
523 while positive values on the x-axes indicate an increase in the average temperature relative
524 to the long-term average. Solid line indicates strong evidence of a relationship.

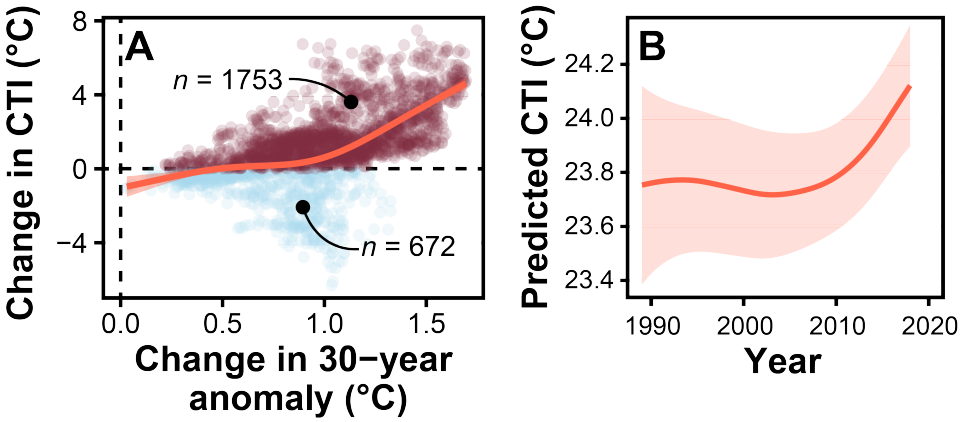

Figure 3: A significant increase in bumble bee CTI is strongly associated with long-term warming and has accelerated in the last 15 years. (A) Biplot of change in 30-year temperature anomaly and change in bumble bee CTI for each grid cell across North America. Trendline is a GAM fit including the 95% confidence interval. Dashed lines indicate no change in anomaly or CTI for the X and Y axes, respectively. (B) Model estimated temporal trend in CTI across North America. Yearly predictions are calculated from the global model for each grid cell, and the trend within each region is illustrated with a GAM fit including the 95% confidence interval.

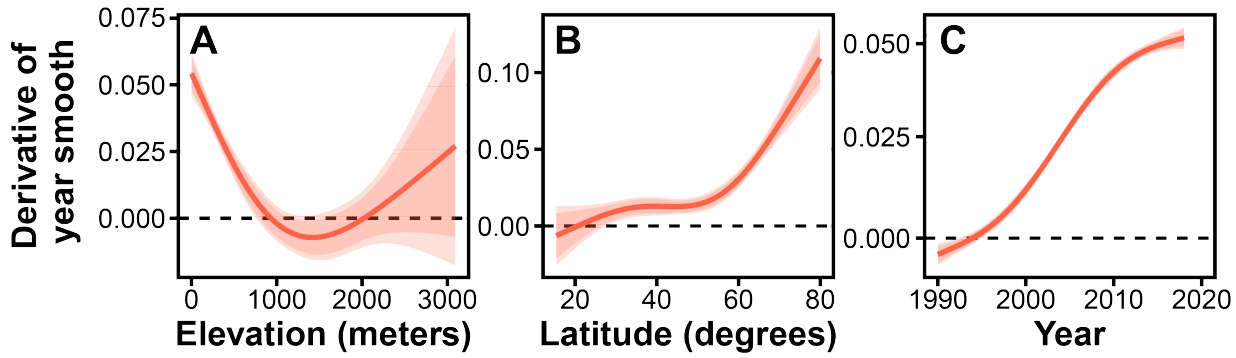

Figure 4: Estimates of the rate of change in CTI over time across (A) elevation, (B) latitude, and (C) year. Yearly predictions of CTI are calculated from the global model for each grid cell using a generalized additive model with a single smooth of year to determine the temporal trend in CTI within the grid cell. For each fitted smooth (except for the year, C), we then calculated the mean derivative across its range (1989-2018) for each grid cell. We then plotted these derivative estimates against elevation and latitude to explore, across the extent of North America, where the rate CTI change is greatest. We visualized the relationships (red lines) using a simple GAM. Model fits include the 95% confidence interval. # References

Supplementary Materials

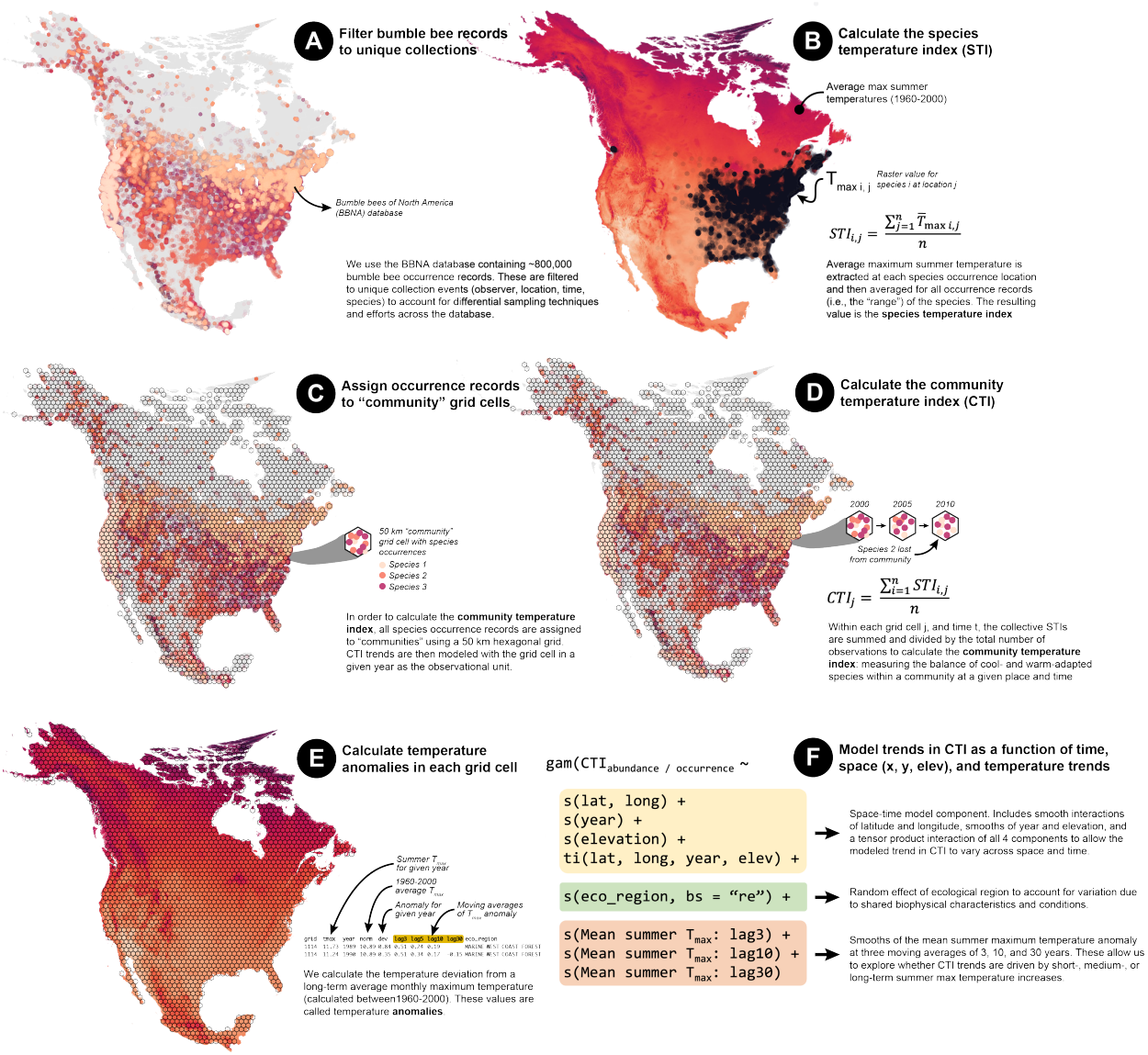

Figure S1: Conceptual figure of data cleaning (A), STI calculation (B), community assignment (C), CTI calculation (D), temperature anomaly calculations (E) and modeling procedures used in our analyses (F).

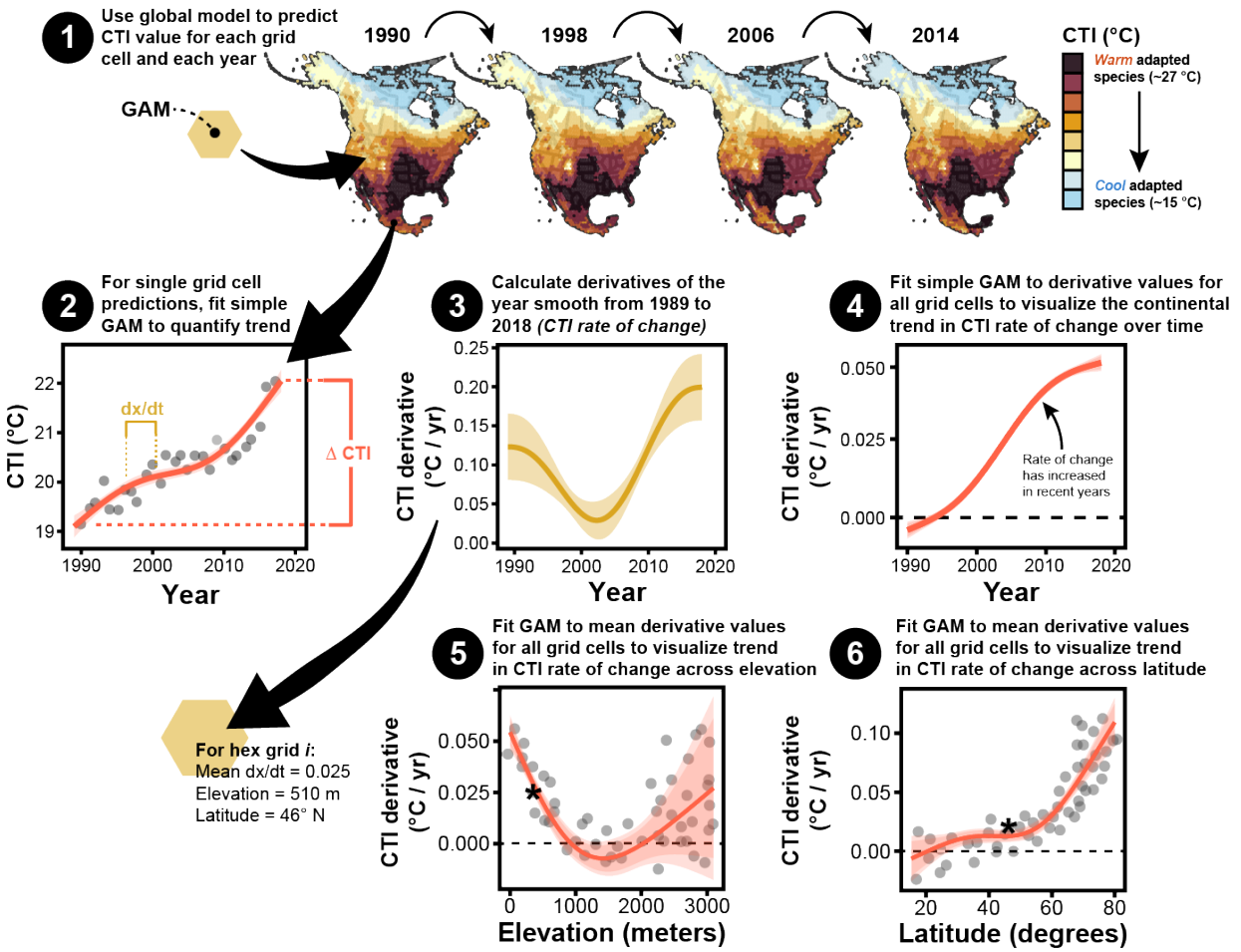

Figure S2: Conceptual diagram of the derivative calculations conducted to determine whether the rate of increase (i.e., derivative) of bumble bee CTI has remained steady or accelerated over space and time. (1) We use the global model to predict the CTI in each grid cell for each year of the study, from 1989-2018. (2) For each grid cell, we fit a GAM through the predicted points to visualize and quantify the trend in CTI from 1989-2018. From these data, we also calculated the change in CTI from 1989-2018 (change in CTI) which is plotted in Fig. 1A. The overall change, however, tells us nothing of the functional form of the relationship between CTI and time, elevation, etc. To address this, we calculated the first derivative across the fitted smooth to determine how the rate of change in CTI varied across time, elevation, and latitude (Fig. 2). (3) For each grid cell's fitted GAM, we calculated the derivative of the year smooth at a range of values between 1989-2018. In this example, because CTI is increasing throughout the entire study period, the derivative is > 0 at all years. (4) We then took the derivative estimates for all grid cells and fit a GAM to visualize the trend between the derivative and time. For elevation (5) and latitude (6), we first averaged the derivative value from 1989-2018 to determine the mean slope for each grid cell before plotting that against the mean elevation and latitude of each grid cell and visualizing the relationship with a GAM. Transparent points are illustrative (not actual values) of individual hex grid derivative values across the range of elevation and latitude. The black star represents a hypothetical mean derivative value from the example plot in (3) to illustrate how mean derivative values are used to assess the trend.

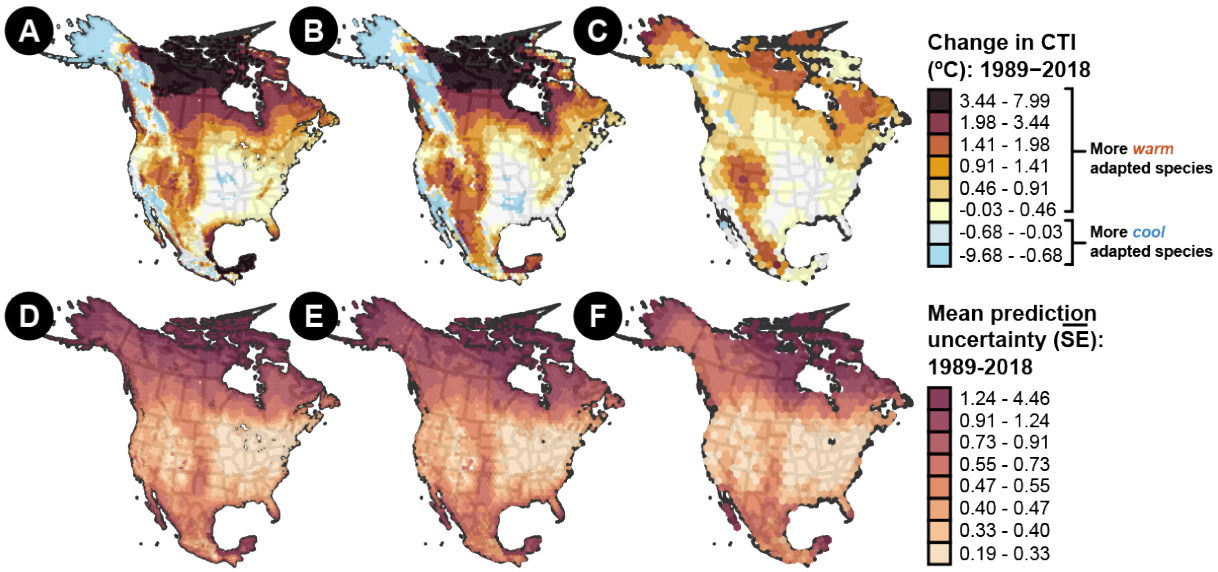

Figure S3: Predicted change in bumble bee CTI across North America between 1989-2018 at three different spatial resolutions of hexagonal grid (distance indicates side-to-side): (A) 50 km; (B) 100 km; (C) 200 km; along with the mean prediction uncertainty at the same resolutions.

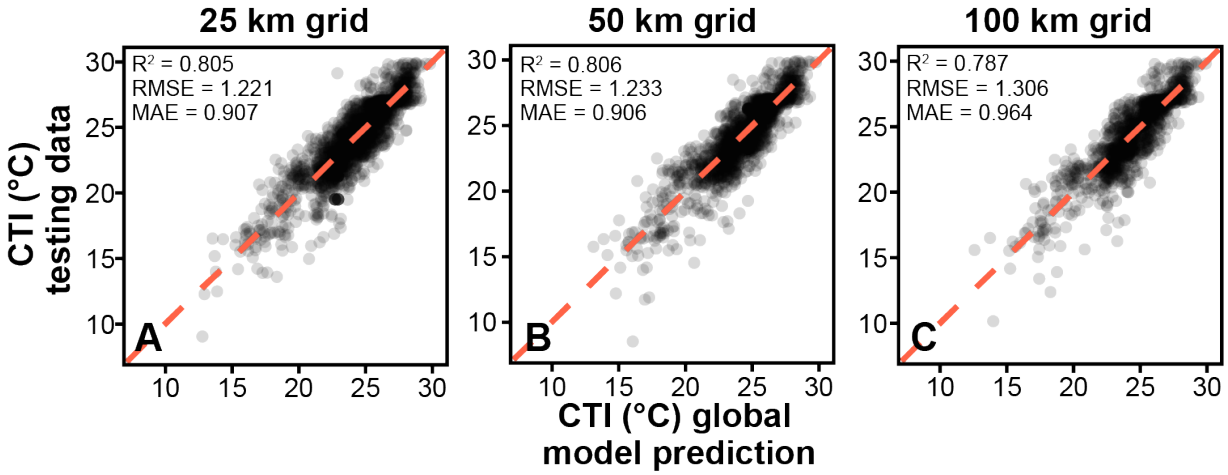

Figure S4: Abundance-weighted global model cross validation results at three different scales of (A) 25 km, (B) 50 km, and (C) 100 km center-to-edge hexagonal grids. Cross validation metrics are given in the top left of each panel including coefficient of determination (R2), root mean squared error (RMSE), and mean absolute error (MAE).

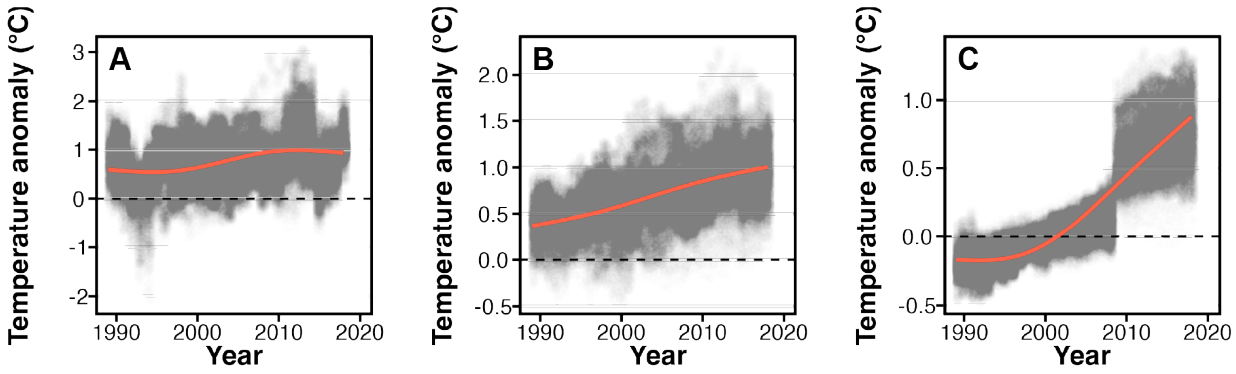

Figure S5: Trend in summer (June – September) maximum temperature anomalies at (A) 3-year, (B) 10-year, and (C) 30-year moving averages. Transparent points are raw values and red lines are GAM trendlines.

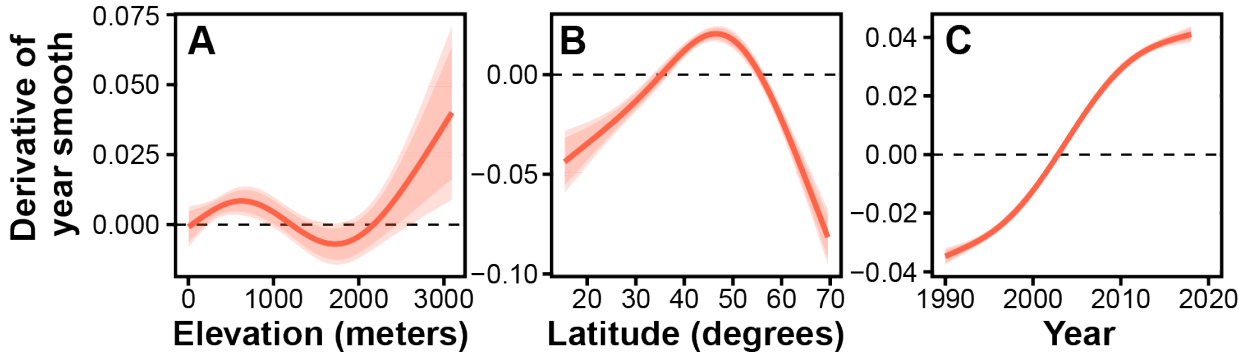

584

585 **Figure S6:** Estimates of the rate of change in CTI over time across (A) elevation, (B)
586 latitude, and (C) year using predictions only from grid cells containing occurrence records
587 (conservative approach). Yearly predictions are calculated from the global model for each
588 grid cell using simple generalized additive models with a single smooth of year to
589 determine CTI trend within the grid cell. For each fitted smooth (except for the year, C), we
590 then calculated the mean derivative across its range (1989-2018) for each grid cell. We
591 then plotted these derivative estimates to explore, across the extent of North America,
592 whether increases in CTI were varied with elevation or over time. We calculated
593 predictions (red lines) from a generalized additive model using a thin-plate basis function
594 and 3 knots for visual purposes only. Estimates include the 95% confidence interval.

595 **Table S1:** Results from a generalized additive model for CTI using occurrence-only and
596 abundance-weighted records from 1989-2018.

	Occurrence model			Abundance model		
Model smooth	**EDF**	**F**	**p value**	**EDF**	**F**	**p value**
Latitude, longitude	282.065	16.778	< 0.001	270.546	18.099	< 0.001
Year	2.945	4.015	0.004	2.353	3.592	0.022
Elevation	7.995	23.926	< 0.001	7.615	25.782	< 0.001
Latitude, longitude, elevation, year	100.149	3.782	< 0.001	97.853	2.996	< 0.001
Ecological region	10.526	2.388	< 0.001	9.855	1.644	< 0.001
Mean Tmax 3-year MA	2.968	2.584	0.032	2.827	2.500	0.039
Mean Tmax 10-year MA	1.002	0.064	0.803	1.001	0.475	0.491
Mean Tmax 30-year MA	2.967	4.561	0.002	3.377	6.712	< 0.001
Model n	5273			5273		
Deviance explained	0.860			0.863		
R-squared (adjusted)	0.849			0.851		

597 *EDF :estimated degrees of freedom (i.e., smooth wiggliness)

598 **Table S2:** Results from a generalized additive model for CTI using occurrence-only records
599 at three different spatial resolutions (community grid scale) at 25, 50, and 100 km from
600 1989-2018.

	25 km grid scale			50 km grid scale			100 km grid scale		
Model smooth	**EDF**	**F**	**p value**	**EDF**	**F**	**p value**	**EDF**	**F**	**p value**
Latitude, longitude	294.224	18.839	< 0.001	270.546	18.099	< 0.001	181.650	17.769	< 0.001
Year	3.653	5.293	< 0.001	2.353	3.592	0.022	2.538	1.609	0.164
Elevation	9.360	34.646	< 0.001	7.615	25.782	< 0.001	1.000	52.860	< 0.001
Latitude, longitude, elevation, year	106.844	4.744	< 0.001	97.853	2.996	< 0.001	51.223	2.558	< 0.001
Ecological region	10.889	4.824	< 0.001	9.855	1.644	< 0.001	11.650	4.843	< 0.001
Mean Tmax 3-year MA	2.881	3.999	0.008	2.827	2.500	0.039	1.000	0.041	0.840
Mean Tmax 10-year MA	1.000	0.061	0.805	1.001	0.475	0.491	3.511	5.344	0.004
Mean Tmax 30-year MA	2.919	5.177	0.001	3.377	6.712	< 0.001	3.029	4.430	0.003
Model n	7582			5273			3078		
Deviance explained	0.840			0.860			0.862		
R-squared (adjusted)	0.831			0.849			0.850		

601 *EDF :estimated degrees of freedom (i.e., smooth wiggliness)

Table S3: Jackknife analysis for both abundance-weighted and occurrence CTI estimates for all species in the dataset. Species temperature index (STI), STI standard deviation, and number of records in the CTI dataset are also given. Percent difference is the difference between the global (including all species) and jackknife model (excluding single species) mean derivative (dx/dt) across the temporal range (1989-2018) of the respective global model. Positive percentages indicate that the species contributes to the CTI trend (i.e., that an increase in abundance/occurrence leads to an increase in CTI).

MOST REPRESENTED SPECIES ***(n records > 1000)***

Species	Subgenus	IUCN redlist category	STI	STI S.D.	Number of records	Global *dx/dt* (abundance)	Global *dx/dt* (occurrence)	Jackknife *dx/dt* (abundance)	Jackknife *dx/dt* (occurrence)	% difference (abundance)	% difference (occurrence)
B. occidentalis	Bombus	Vulnerable	21.688	4.862	2357	0.018	0.018	0.005	0.002	70.424	89.202
B. nevadensis	Bombias	Least Concern	24.539	4.102	2236	0.018	0.015	0.005	0.003	69.653	81.752
B. ephippiatus	Pyrobombus	Least Concern	23.715	3.426	3153	0.023	0.021	0.008	0.005	66.868	75.315
B. bifarius	Pyrobombus	Least Concern	22.023	4.132	3237	0.024	0.023	0.008	0.007	66.716	69.324
B. vosnesenskii	Pyrobombus	Least Concern	25.585	4.016	7514	0.025	0.021	0.009	0.008	64.318	63.772
B. huntii	Pyrobombus	Least Concern	25.764	3.066	4556	0.019	0.016	0.007	0.004	64.161	72.12
B. impatiens	Pyrobombus	Least Concern	27.019	2.507	52373	0.021	0.015	0.008	0.005	62.382	63.191
B. appositus	Subterraneobombus	Least Concern	22.644	3.263	1204	0.03	0.024	0.013	0.009	55.057	60.367
B. centralis	Pyrobombus	Least Concern	23.806	3.602	1991	0.016	0.014	0.008	0.006	50.166	58.733
B. pensylvanicus	Thoracobombus	Vulnerable	29.817	3.057	16763	0.019	0.012	0.01	0.006	44.172	51.223
B. flavifrons	Pyrobombus	Least Concern	20.427	4.126	3274	0.03	0.028	0.018	0.015	40.272	44.577
B. griseocollis	Cullumanobombus	Least Concern	27.017	2.306	21310	0.033	0.027	0.02	0.014	38.469	47.951
B. sylvicola	Pyrobombus	Least Concern	17.018	4.312	1093	0.049	0.044	0.031	0.028	35.224	37.181
B. auricomus	Bombias	Least Concern	27.586	1.834	3172	0.018	0.012	0.012	0.007	35.221	40.898
B. insularis	Psithyrus	Least Concern	22.194	3.755	1415	0.026	0.022	0.017	0.013	34.774	40.71
B. melanopygus	Pyrobombus	Least Concern	22.486	5.575	5054	0.036	0.031	0.023	0.019	34.355	36.794
B. bimaculatus	Pyrobombus	Least Concern	26.563	2.086	13788	0.016	0.009	0.01	0.005	33.454	40.704
B. fervidus	Thoracobombus	Vulnerable	25.637	2.887	7192	0.027	0.022	0.018	0.013	32.296	39.02
B. frigidus	Pyrobombus	Least Concern	16.409	5.531	1043	0.042	0.038	0.028	0.024	32.164	36.044
B. terricola	Bombus	Vulnerable	22.795	1.987	3905	0.038	0.032	0.026	0.021	31.586	34.711
B. flavidus	Psithyrus	Data Deficient	20.051	2.875	1242	0.039	0.034	0.029	0.025	25.842	27.554
B. perplexus	Pyrobombus	Least Concern	23.724	2.571	4428	0.043	0.037	0.032	0.026	25.713	29.98
B. rufocinctus	Cullumanobombus	Least Concern	23.628	2.739	5306	0.028	0.023	0.022	0.017	24.284	27.606
B. vagans	Pyrobombus	Least Concern	24.615	2.401	7713	0.027	0.021	0.022	0.017	18.602	20.168
B. mixtus	Pyrobombus	Least Concern	20.269	5.038	3628	0.044	0.04	0.037	0.031	16.611	22.522
B. borealis	Subterraneobombus	Least Concern	22.960	1.999	3355	0.033	0.028	0.031	0.026	7.942	8.631
B. citrinus	Psithyrus	Least Concern	25.139	2.138	2229	0.032	0.024	0.031	0.023	2.711	1.935
B. affinis	Bombus	Critically Endangered	25.511	1.710	2188	0.016	0.007	0.016	0.009	-4.755	-24.531
B. ternarius	Pyrobombus	Least Concern	22.954	1.731	10215	0.036	0.03	0.039	0.03	-7.966	-1.741

LESS REPRESENTED SPECIES ***(n records < 1000)***

Species	Subgenus	IUCN redlist category	STI	STI S.D.	Number of records	Global *dx/dt* (abundance)	Global *dx/dt* (occurrence)	Jackknife *dx/dt* (abundance)	Jackknife *dx/dt* (occurrence)	% difference (abundance)	% difference (occurrence)
B. macgregori	Cullumanobombus	Least Concern	22.475	0.000	71	0	0.003	0.001	-0.007	1781.842	331.519
B. trinominatus	Thoracobombus	Least Concern	16.550	0.328	223	0.005	0.005	-0.004	-0.005	180.522	196.414
B. steindachneri	Thoracobombus	Endangered	28.613	3.072	321	0.016	0.017	-0.003	-0.002	118.408	110.735
B. haueri	Cullumanobombus	Endangered	22.698	3.456	45	0.024	0.024	-0.001	-0.001	104.39	104.082
B. brachycephalus	Cullumanobombus	Endangered	25.308	1.878	96	0.015	0.013	0	-0.001	102.073	110.963
B. weisi	Thoracobombus	Least Concern	22.650	2.167	994	0.016	0.015	0.001	0	95.591	97.538
B. mexicanus	Thoracobombus	Vulnerable	29.125	3.111	94	0.016	0.013	0.001	-0.001	91.596	107.946
B. diligens	Thoracobombus	Near Threatened	26.415	2.185	334	0.023	0.02	0.002	0.002	91.55	91.555
B. jonellus	Pyrobombus	Data Deficient	16.233	2.632	359	0.028	0.033	0.006	0.009	78.321	74.001
B. caliginosus	Pyrobombus	Vulnerable	23.542	3.050	282	0.014	0.008	0.003	0	78.248	102.669
B. fraternus	Cullumanobombus	Endangered	30.611	2.308	927	0.007	0.002	0.002	-0.001	78.176	172.649
B. medius	Thoracobombus	Vulnerable	28.500	2.486	609	0.029	0.021	0.009	0.004	70.17	82.763
B. vandykei	Pyrobombus	Least Concern	27.423	4.228	464	0.018	0.012	0.006	0.002	69.842	87.082
B. cryptarum	Bombus	Data Deficient	7.373	6.161	779	0.028	0.032	0.008	0.008	69.7	75.074
B. neoboreus	Alpinobombus	Data Deficient	7.884	6.184	43	0.056	0.056	0.022	0.022	61.607	61.048
B. variabilis	Psithyrus	Critically Endangered	29.661	2.587	92	0.017	0.01	0.007	0.003	59.301	73.525
B. franklini	Bombus	Critically Endangered	25.076	4.501	64	0.012	0.005	0.006	0.002	53.69	55.804
B. kirbiellus	Alpinobombus	Data Deficient	14.843	5.930	280	0.039	0.038	0.023	0.02	42.119	45.946
B. polaris	Alpinobombus	Data Deficient	9.753	5.012	96	0.06	0.057	0.038	0.032	36.908	43.165
B. natvigi	Alpinobombus	Data Deficient	7.473	5.901	16	0.075	0.071	0.048	0.038	35.874	46.663
B. morrisoni	Cullumanobombus	Vulnerable	27.991	3.534	489	0.035	0.028	0.024	0.019	30.837	31.588
B. pullatus	Thoracobombus	Data Deficient	30.905	0.253	41	0.039	0.023	0.028	0.021	27.867	8.659
B. suckleyi	Psithyrus	Critically Endangered	22.644	3.220	86	0.048	0.042	0.036	0.03	24.935	28.31
B. bohemicus	Psithyrus	Data Deficient	22.839	2.339	320	0.043	0.038	0.033	0.028	23.413	27.549
B. sandersoni	Pyrobombus	Least Concern	22.221	2.361	765	0.044	0.037	0.038	0.031	13.727	14.44
B. sitkensis	Pyrobombus	Least Concern	21.060	3.909	534	-0.005	-0.003	-0.007	-0.006	-27.155	-124.088

References

Bartomeus, I., Ascher, J. S., Wagner, D., Danforth, B. N., Colla, S., Kornbluth, S., & Winfree, R. (2011). Climate-associated phenological advances in bee pollinators and bee-pollinated plants. *Proceedings of the National Academy of Sciences*, *108*(51), 20645–20649. https://doi.org/10.1073/pnas.1115559108

Bartomeus, I., Stavert, J. R., Ward, D., & Aguado, O. (2019). Historical collections as a tool for assessing the global pollination crisis. *Philosophical Transactions of the Royal Society B*, *374*(1763), 20170389. https://doi.org/10.1098/rstb.2017.0389

Birch, C. P. D., Oom, S. P., & Beecham, J. A. (2007). Rectangular and hexagonal grids used for observation, experiment and simulation in ecology. *Ecological Modelling*, *206*(3-4), 347–359. https://doi.org/10.1016/j.ecolmodel.2007.03.041

Cameron, S. A., Lozier, J. D., Strange, J. P., Koch, J. B., Cordes, N., Solter, L. F., & Griswold, T. L. (2011). Patterns of widespread decline in North American bumble bees. *Proceedings of the National Academy of Sciences*, *108*(2), 662–667. https://doi.org/10.1073/pnas.1014743108

CaraDonna, P. J., Cunningham, J. L., & Iler, A. M. (2018). Experimental warming in the field delays phenology and reduces body mass, fat content and survival: Implications for the persistence of a pollinator under climate change. *Functional Ecology*, *32*(10), 2345–2356. https://doi.org/10.1111/1365-2435.13151

Colla, S. R., Otterstatter, M. C., Gegear, R. J., & Thomson, J. D. (2006). Plight of the bumble bee: Pathogen spillover from commercial to wild populations. *Biological Conservation*, *129*(4), 461–467. https://doi.org/10.1016/j.biocon.2005.11.013

Crossley, M. S., Smith, O. M., Berry, L. L., Phillips-Cosio, R., Glassberg, J., Holman, K. M., Holmquest, J. G., Meier, A. R., Varriano, S. A., McClung, M. R., Moran, M. D., & Snyder, W. E. (2021). Recent climate change is creating hotspots of butterfly increase and decline across North America. *Global Change Biology*, *27*(12), 2702–2714. https://doi.org/10.1111/gcb.15582

Daniel Baston. (2022). *Exactextractr: Fast extraction from raster datasets using polygons*. https://CRAN.R-project.org/package=exactextractr

Devictor, V., Julliard, R., Couvet, D., & Jiguet, F. (2008). Birds are tracking climate warming, but not fast enough. *Proceedings of the Royal Society B: Biological Sciences*, *275*(1652), 2743–2748. https://doi.org/10.1098/rspb.2008.0878

Devictor, V., Swaay, C. van, Brereton, T., Brotons, L., Chamberlain, D., Heliölä, J., Herrando, S., Julliard, R., Kuussaari, M., Lindström, Å., Reif, J., Roy, D. B., Schweiger, O., Settele, J., Stefanescu, C., Strien, A. V., Turnhout, C. V., Vermouzek, Z., WallisDeVries, M., … Jiguet, F. (2012). Differences in the climatic debts of birds and butterflies at a continental scale. *Nature Climate Change*, *2*(2), 121–124. https://doi.org/10.1038/nclimate1347

Dillon, M. E., Wang, G., & Huey, R. B. (2010). Global metabolic impacts of recent climate warming. *Nature*, *467*(7316), 704–706. https://doi.org/10.1038/nature09407

649 Dowle, M., & Srinivasan, A. (2023). *Data.table: Extension of 'data.frame'*. https://CRAN.R-
650 project.org/package=data.table

651 Duchenne, F., Thébault, E., Michez, D., Gérard, M., Devaux, C., Rasmont, P., Vereecken, N. J., &
652 Fontaine, C. (2020). Long-term effects of global change on occupancy and flight period of
653 wild bees in Belgium. *Global Change Biology*. https://doi.org/10.1111/gcb.15379

654 Engelhardt, E. K., Biber, M. F., Dolek, M., Fartmann, T., Hochkirch, A., Leidinger, J., Löffler, F.,
655 Pinkert, S., Poniatowski, D., Voith, J., Winterholler, M., Zeuss, D., Bowler, D. E., & Hof, C.
656 (2022). Consistent signals of a warming climate in occupancy changes of three insect taxa
657 over 40 years in central Europe. *Global Change Biology*, *28*(13), 3998–4012.
658 https://doi.org/10.1111/gcb.16200

659 Fick, S. E., & Hijmans, R. J. (2017). WorldClim 2: new 1km spatial resolution climate
660 surfaces for global land areas. *International Journal of Climatology*, *12*(37), 4302–4315.
661 https://doi.org/10.1111/gcb.15379

662 Fijen, T. P. M. (2021). Mass-migrating bumblebees: An overlooked phenomenon with
663 potential far-reaching implications for bumblebee conservation. *Journal of Applied Ecology*,
664 *58*(2), 274–280. https://doi.org/10.1111/1365-2664.13768

665 Firke, S. (2021). *Janitor: Simple tools for examining and cleaning dirty data*. https://CRAN.R-
666 project.org/package=janitor

667 Fourcade, Y., Åström, S., & Öckinger, E. (2019). Climate and land-cover change alter
668 bumblebee species richness and community composition in subalpine areas. *Biodiversity*
669 *and Conservation*, *28*(3), 639–653. https://doi.org/10.1007/s10531-018-1680-1

670 Gotelli, N. J., Booher, D. B., Urban, M. C., Ulrich, W., Suarez, A. V., Skelly, D. K., Russell, D. J.,
671 Rowe, R. J., Rothendler, M., Rios, N., Rehan, S. M., Ni, G., Moreau, C. S., Magurran, A. E., Jones,
672 F. A. M., Graves, G. R., Fiera, C., Burkhardt, U., & Primack, R. B. (2021). Estimating species
673 relative abundances from museum records. *Methods in Ecology and Evolution*.
674 https://doi.org/10.1111/2041-210x.13705

675 Guzman, L. M., Johnson, S. A., Mooers, A. O., & M'Gonigle, L. K. (2021). Using historical data
676 to estimate bumble bee occurrence: Variable trends across species provide little support
677 for community-level declines. *Biological Conservation*, *257*, 109141.
678 https://doi.org/10.1016/j.biocon.2021.109141

679 Halsch, C. A., Shapiro, A. M., Fordyce, J. A., Nice, C. C., Thorne, J. H., Waetjen, D. P., & Forister,
680 M. L. (2021). Insects and recent climate change. *Proceedings of the National Academy of*
681 *Sciences*, *118*(2), e2002543117. https://doi.org/10.1073/pnas.2002543117

682 Hartig, F. (2022). *DHARMa: Residual diagnostics for hierarchical (multi-level / mixed)*
683 *regression models*. https://CRAN.R-project.org/package=DHARMa

684 Hemberger, J. A., Rosenberger, N. M., & Williams, N. M. (2023). Experimental heatwaves
685 disrupt bumblebee foraging through direct heat effects and reduced nectar production.
686 *Functional Ecology*, *37*(3), 591–601. https://doi.org/10.1111/1365-2435.14241

687 Hemberger, J., Crossley, M. S., & Gratton, C. (2021). Historical decrease in agricultural
688 landscape diversity is associated with shifts in bumble bee species occurrence. *Ecology*
689 *Letters*, *24*(9), 1800–1813. https://doi.org/10.1111/ele.13786

690 Hijmans, R. J. (2023). *Raster: Geographic data analysis and modeling*. https://CRAN.R-
691 project.org/package=raster

692 Hoover, S. E. R., Ladley, J. J., Shchepetkina, A. A., Tisch, M., Gieseg, S. P., & Tylianakis, J. M.
693 (2012). Warming, CO2, and nitrogen deposition interactively affect a plant-pollinator
694 mutualism. *Ecology Letters*, *15*(3), 227–234. https://doi.org/10.1111/j.1461-
695 0248.2011.01729.x

696 Høye, T. T., Loboda, S., Koltz, A. M., Gillespie, M. A. K., Bowden, J. J., & Schmidt, N. M. (2021).
697 Nonlinear trends in abundance and diversity and complex responses to climate change in
698 Arctic arthropods. *Proceedings of the National Academy of Sciences*, *118*(2), e2002557117.
699 https://doi.org/10.1073/pnas.2002557117

700 Hvitfeldt, E. (2021). *Paletteer: Comprehensive collection of color palettes*.
701 https://github.com/EmilHvitfeldt/paletteer

702 Iserbyt, S., & Rasmont, P. (2013). The effect of climatic variation on abundance and
703 diversity of bumblebees: a ten years survey in a mountain hotspot. *Annales de La Société*
704 *Entomologique de France (N.S.)*, *48*(3-4), 261–273.
705 https://doi.org/10.1080/00379271.2012.10697775

706 Jackson, H. M., Johnson, S. A., Morandin, L. A., Richardson, L. L., Guzman, L. M., & M'Gonigle,
707 L. K. (2022). Climate change winners and losers among North American bumblebees.
708 *Biology Letters*, *18*(6), 20210551. https://doi.org/10.1098/rsbl.2021.0551

709 Janousek, W. M., Douglas, M. R., Cannings, S., Clément, M. A., Delphia, C. M., Everett, J. G.,
710 Hatfield, R. G., Keinath, D. A., Koch, J. B. U., McCabe, L. M., Mola, J. M., Ogilvie, J. E., Rangwala,
711 I., Richardson, L. L., Rohde, A. T., Strange, J. P., Tronstad, L. M., & Graves, T. A. (2023). Recent
712 and future declines of a historically widespread pollinator linked to climate, land cover, and
713 pesticides. *Proceedings of the National Academy of Sciences*, *120*(5).
714 https://doi.org/10.1073/pnas.2211223120

715 Johnson, M. G., Glass, J. R., Dillon, M. E., & Harrison, J. F. (2023). How will climatic warming
716 affect insect pollinators? *Advances in Insect Physiology*.
717 https://doi.org/10.1016/bs.aiip.2023.01.001

718 Kammerer, M., Goslee, S. C., Douglas, M. R., Tooker, J. F., & Grozinger, C. M. (2021). Wild bees
719 as winners and losers: Relative impacts of landscape composition, quality, and climate.
720 *Global Change Biology*. https://doi.org/10.1111/gcb.15485

721 Kenna, D., Graystock, P., & Gill, R. J. (2023). Toxic temperatures: Bee behaviours exhibit
722 divergent pesticide toxicity relationships with warming. *Global Change Biology*.
723 https://doi.org/10.1111/gcb.16671

724 Kenna, D., Pawar, S., & Gill, R. J. (2021). Thermal flight performance reveals impact of
725 warming on bumblebee foraging potential. *Functional Ecology*.
726 https://doi.org/10.1111/1365-2435.13887

727 Kerr, J. T., Pindar, A., Galpern, P., Packer, L., Potts, S. G., Roberts, S. M., Rasmont, P.,
728 Schweiger, O., Colla, S. R., Richardson, L. L., Wagner, D. L., Gall, L. F., Sikes, D. S., & Pantoja, A.
729 (2015). Climate change impacts on bumblebees converge across continents. *Science*,
730 *349*(6244), 177–180. https://doi.org/10.1126/science.aaa7031

731 Kim, H., McComb, B. C., Frey, S. J. K., Bell, D. M., & Betts, M. G. (2022). Forest microclimate
732 and composition mediate long-term trends of breeding bird populations. *Global Change*
733 *Biology*, *28*(21), 6180–6193. https://doi.org/10.1111/gcb.16353

734 Lehmann, P., Ammunét, T., Barton, M., Battisti, A., Eigenbrode, S. D., Jepsen, J. U., Kalinkat, G.,
735 Neuvonen, S., Niemelä, P., Terblanche, J. S., Økland, B., & Björkman, C. (2020). Complex
736 responses of global insect pests to climate warming. *Frontiers in Ecology and the*
737 *Environment*, *18*(3), 141–150. https://doi.org/10.1002/fee.2160

738 Looney, C., Strange, J. P., Freeman, M., & Jennings, D. (2019). The expanding Pacific
739 Northwest range of Bombus impatiens Cresson and its establishment in Washington State.
740 *Biological Invasions*, *21*(6), 1879–1885. https://doi.org/10.1007/s10530-019-01970-6

741 Lopez, H., West, R., Dong, S., Goni, G., Kirtman, B., Lee, S.-K., & Atlas, R. (2018). Early
742 emergence of anthropogenically forced heat waves in the western United States and Great
743 Lakes. *Nature Climate Change*, *8*(5), 414–420. https://doi.org/10.1038/s41558-018-0116-
744 y

745 Lüdecke, D., Ben-Shachar, M. S., Patil, I., Waggoner, P., & Makowski, D. (2021). performance:
746 An R package for assessment, comparison and testing of statistical models. *Journal of Open*
747 *Source Software*, *6*(60), 3139. https://doi.org/10.21105/joss.03139

748 Maebe, K., Hart, A. F., Marshall, L., Vandamme, P., Vereecken, N. J., Michez, D., & Smagghe, G.
749 (2021). Bumblebee resilience to climate change, through plastic and adaptive responses.
750 *Global Change Biology*, *27*(18), 4223–4237. https://doi.org/10.1111/gcb.15751

751 Maron, M., McAlpine, C. A., Watson, J. E. M., Maxwell, S., & Barnard, P. (2015). Climate-
752 induced resource bottlenecks exacerbate species vulnerability: a review. *Diversity and*
753 *Distributions*, *21*(7), 731–743. https://doi.org/10.1111/ddi.12339

754 Meehl, G. A., & Tebaldi, C. (2004). More Intense, More Frequent, and Longer Lasting Heat
755 Waves in the 21st Century. *Science*, *305*(5686), 994–997.
756 https://doi.org/10.1126/science.1098704

757 Microsoft, & Weston, S. (2022). *Foreach: Provides foreach looping construct*.
758 https://CRAN.R-project.org/package=foreach

759 Neff, F., Korner-Nievergelt, F., Rey, E., Albrecht, M., Bollmann, K., Cahenzli, F., Chittaro, Y.,
760 Gossner, M. M., Martínez-Núñez, C., Meier, E. S., Monnerat, C., Moretti, M., Roth, T., Herzog,
761 F., & Knop, E. (2022). Different roles of concurring climate and regional land-use changes in
762 past 40 years' insect trends. *Nature Communications*, *13*(1), 7611.
763 https://doi.org/10.1038/s41467-022-35223-3

764 Ockendon, N., Baker, D. J., Carr, J. A., White, E. C., Almond, R. E. A., Amano, T., Bertram, E.,
765 Bradbury, R. B., Bradley, C., Butchart, S. H. M., Doswald, N., Foden, W., Gill, D. J. C., Green, R.
766 E., Sutherland, W. J., Tanner, E. V. J., & Pearce-Higgins, J. W. (2014). Mechanisms
767 underpinning climatic impacts on natural populations: altered species interactions are

768 more important than direct effects. *Global Change Biology*, *20*(7), 2221–2229.
769 https://doi.org/10.1111/gcb.12559

770 Ogilvie, J. E., Griffin, S. R., Gezon, Z. J., Inouye, B. D., Underwood, N., Inouye, D. W., & Irwin, R.
771 E. (2017). Interannual bumble bee abundance is driven by indirect climate effects on floral
772 resource phenology. *Ecology Letters*, *20*(12), 1507–1515.
773 https://doi.org/10.1111/ele.12854

774 Oliver, I., Dorrough, J., Doherty, H., & Andrew, N. R. (2016). Additive and synergistic effects
775 of land cover, land use and climate on insect biodiversity. *Landscape Ecology*, *31*(10), 2415–
776 2431. https://doi.org/10.1007/s10980-016-0411-9

777 Oliver, T. H., Marshall, H. H., Morecroft, M. D., Brereton, T., Prudhomme, C., & Huntingford, C.
778 (2015). Interacting effects of climate change and habitat fragmentation on drought-
779 sensitive butterflies. *Nature Climate Change*, *5*(10), 941–945.
780 https://doi.org/10.1038/nclimate2746

781 Outhwaite, C. L., McCann, P., & Newbold, T. (2022). Agriculture and climate change are
782 reshaping insect biodiversity worldwide. *Nature*, 1–6. https://doi.org/10.1038/s41586-
783 022-04644-x

784 Oyen, K. J., Giri, S. & Dillon, M. E. (2016). Altitudinal variation in bumble bee (Bombus)
785 critical thermal limits. *J Therm Biol* 59, 52–57.
786 https://doi.org/10.1016/j.jtherbio.2016.04.015

787 Palmier, K., Sheffield, C., & Sheffield, C. (2019). First records of the Common Eastern
788 Bumble Bee, Bombus impatiens Cresson (Hymenoptera: Apidae, Apinae, Bombini) from the
789 Prairies Ecozone in Canada. *Biodiversity Data Journal*, *7*(7), e30953.
790 https://doi.org/10.3897/bdj.7.e30953

791 PARMESAN, C. (2007). Influences of species, latitudes and methodologies on estimates of
792 phenological response to global warming. *Global Change Biology*, *13*(9), 1860–1872.
793 https://doi.org/10.1111/j.1365-2486.2007.01404.x

794 Pebesma, E. (2018). Simple Features for R: Standardized Support for Spatial Vector Data.
795 *The R Journal*, *10*(1), 439–446. https://doi.org/10.32614/RJ-2018-009

796 Pedersen, E. J., Miller, D. L., Simpson, G. L., & Ross, N. (2019). Hierarchical generalized
797 additive models in ecology: an introduction with mgcv. *PeerJ*, *7*, e6876.
798 https://doi.org/10.7717/peerj.6876

799 Pincebourde, S., & Woods, H. A. (2020). There is plenty of room at the bottom:
800 microclimates drive insect vulnerability to climate change. *Current Opinion in Insect*
801 *Science*, *41*, 63–70. https://doi.org/10.1016/j.cois.2020.07.001

802 Princé, K., & Zuckerberg, B. (2015). Climate change in our backyards: the reshuffling of
803 North America's winter bird communities. *Global Change Biology*, *21*(2), 572–585.
804 https://doi.org/10.1111/gcb.12740

805 Pyke, G. H., Thomson, J. D., Inouye, D. W., & Miller, T. J. (2016). Effects of climate change on
806 phenologies and distributions of bumble bees and the plants they visit. *Ecosphere*, *7*(3).
807 https://doi.org/10.1002/ecs2.1267

R Core Team. (2017). *R: A language and environment for statistical computing*. R Foundation for Statistical Computing. https://www.R-project.org/

Raven, P. H., & Wagner, D. L. (2021). Agricultural intensification and climate change are rapidly decreasing insect biodiversity. *Proceedings of the National Academy of Sciences*, *118*(2), e2002548117. https://doi.org/10.1073/pnas.2002548117

Richardson, L. et al., (2023). Bumble Bees of North America (https://www.leifrichardson.org/bbna.html)

Settele, J., Bishop, J., & Potts, S. G. (2016). Climate change impacts on pollination. *Nature Plants*, *2*(7), 16092. https://doi.org/10.1038/nplants.2016.92

Simpson, G. L. (2018). Modelling Palaeoecological Time Series Using Generalised Additive Models. *Frontiers in Ecology and Evolution*, *6*, 149. https://doi.org/10.3389/fevo.2018.00149

Simpson, G. L. (2023). *gratia: Graceful ggplot-based graphics and other functions for GAMs fitted using mgcv*. https://gavinsimpson.github.io/gratia/

Sirois-Delisle, C., & Kerr, J. T. (2018). Climate change-driven range losses among bumblebee species are poised to accelerate. *Scientific Reports*, *8*(1), 14464. https://doi.org/10.1038/s41598-018-32665-y

Soroye, P., Newbold, T., & Kerr, J. (2020). Climate change contributes to widespread declines among bumble bees across continents. *Science*, *367*(6478), 685–688. https://doi.org/10.1126/science.aax8591

Szabo, N. D., Colla, S. R., Wagner, D. L., Gall, L. F., & Kerr, J. T. (2012). Do pathogen spillover, pesticide use, or habitat loss explain recent North American bumblebee declines?: Causes of bumblebee declines. *Conservation Letters*, *5*(3), 232–239. https://doi.org/10.1111/j.1755-263x.2012.00234.x

Thompson, V., Kennedy-Asser, A. T., Vosper, E., Lo, Y. T. E., Huntingford, C., Andrews, O., Collins, M., Hegerl, G. C., & Mitchell, D. (2022). The 2021 western North America heat wave among the most extreme events ever recorded globally. *Science Advances*, *8*(18), eabm6860. https://doi.org/10.1126/sciadv.abm6860

Tingley, M. W., & Beissinger, S. R. (2013). Cryptic loss of montane avian richness and high community turnover over 100 years. *Ecology*, *94*(3), 598–609. https://doi.org/10.1890/12-0928.1

Warren, M. S., Hill, J. K., Thomas, J. A., Asher, J., Fox, R., Huntley, B., Roy, D. B., Telfer, M. G., Jeffcoate, S., Harding, P., Jeffcoate, G., Willis, S. G., Greatorex-Davies, J. N., Moss, D., & Thomas, C. D. (2001). Rapid responses of British butterflies to opposing forces of climate and habitat change. *Nature*, *414*(6859), 65–69. https://doi.org/10.1038/35102054

Whitehorn, P. R., Seo, B., Comont, R. F., Rounsevell, M., & Brown, C. (2022). The effects of climate and land use on British bumblebees: Findings from a decade of citizen-science observations. *Journal of Applied Ecology*, *59*(7), 1837–1851. https://doi.org/10.1111/1365-2664.14191

847 Wickham, H., Averick, M., Bryan, J., Chang, W., McGowan, L. D., François, R., Grolemund, G.,
848 Hayes, A., Henry, L., Hester, J., Kuhn, M., Pedersen, T. L., Miller, E., Bache, S. M., Müller, K.,
849 Ooms, J., Robinson, D., Seidel, D. P., Spinu, V., … Yutani, H. (2019). Welcome to the tidyverse.
850 *Journal of Open Source Software*, *4*(43), 1686. https://doi.org/10.21105/joss.01686

851 Wood, S. N. (2011). Fast stable restricted maximum likelihood and marginal likelihood
852 estimation of semiparametric generalized linear models. *Journal of the Royal Statistical*
853 *Society (B)*, *73*(1), 3–36.